Conception and evaluation of a musculoskeletal finite element model of the lumbar spine

Marie Line Pissonnier, Antoine Perrier, Marek Bucki, Jerome Tonetti, Yohan Payan, Robert Carlier

Conception and evaluation of a musculoskeletal finite element model of the lumbar spine

Marie Line Pissonnier *
TIMC Laboratory, Biomeca Team, Grenoble Alpes University, France

Antoine Perrier
TIMC Laboratory, Biomeca Team, Grenoble Alpes University, France
TwInsight, Grenoble, France

Marek Bucki
TwInsight, Grenoble, France

Jerome Tonetti
Orthopaedic Surgery Department, Grenoble University Hospitals, France

Robert Carlier
Medical Imaging Department, Raymond Poincare Hospital, APHP, Garches, France

Yohan Payan
TIMC Laboratory, Biomeca Team, Grenoble Alpes University, France

***Corresponding author.** Email: ml.pissonnier@gmail.com

Keywords: lumbar spine; hybrid model; multi-position MRI

1. Introduction

Many spinal pathologies can result in soft tissue and/or bone damage, leading to loss of mobility or, conversely, instability of one or more segments.
The aim of human spine modeling is to use computer simulation to help clinicians understand the pathophysiology of the spine and evaluate different treatment options.
This work aims to develop a patient-specific multi-bodies and finite element model of the lumbar spine, as a continuation of the lower limb modeling project initiated in the TIMC laboratory. (Perrier et al. 2015; Elyasi et al. 2022)

2. Methods

2.1 Conception of the model *(figure 1 A &B)*
Radiological data (CT scan, MRI) from a healthy 36-year-old man were collected retrospectively after consent was obtained for this study. Bones, muscles, and ligaments of interest were segmented using Amira software (thermofisher.com). The thoraco-lumbar spine model was developed using the Artisynth 3D biomechanical simulation platform (artisynth.org). It includes 17 intervertebral discs modeled using 2-domain hexahedral finite elements (annulus and nucleus), 53 bones (including 17 vertebrae) modeled as rigid bodies connected by 940 cables simulating the 11 groups of ligaments in their real position and thus defining joints with contact. Ligament and capsular material properties were implemented according to Goel et al (1995). The thoracolumbar fascia (TLF) is modeled by shell elements connected to the bones or muscles. A set of 15 muscles (represented by around 500 1D deformable fibers) is positioned anatomically. Via points along the muscle paths were created to correlate with actual muscle volume and torsion. Anatomical structures not visible on the images were implemented in accordance with anatomical reference works such as the book from Bogduk (2013). This study focuses on the lumbar part.

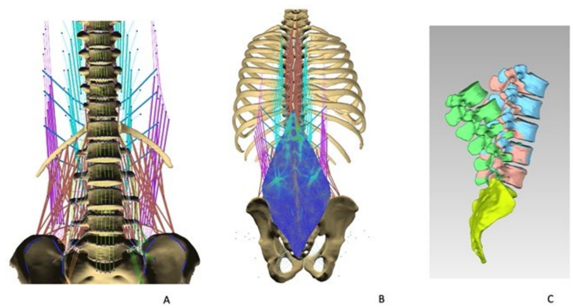

Figure 1. *Musculoskeletal model with ligaments and muscular paths. A. Anterior view, B. Posterior view with TLF. C. Registrated lumbar vertebrae in multiple positions.*
credit: A.Perrier

2.2 Kinematic evaluation of the lumbar part
To evaluate the kinematic accuracy of the model created from supine data, a method using sitting upright MRI in neutral, extreme flexion and extension positions was developed. In this study we compared the sagittal parameters measured on the MRIs with the same parameters extracted at specific poses during a simulation of flexion and extension.

Bones from L1 to the sacrum were segmented based on the MRIs in the three positions. Intervertebral angles and lumbar lordosis (from L1 to L5) were manually calculated in those positions in accordance with Cobb technique defined on 2D X-rays, as described as disc wedging angle by Modi (2008) and reported as aMRI in table 1.

The CT scan vertebrae were registered with the MRI ones to have a better precision on the zygapophyseal joints. The non interpenetration of the vertebrae was checked, and to assess the registration, same measurements were performed (aReg in table 1). Figure 1C plots the 3 registered lumbar spines in MRI positions.

The simulation of flexion is performed under force displacement. A 200N 3D vector was applied to the L1 spinous process on the vertebra's sagittal plane, in a direction perpendicular to the posterior wall of the vertebra. The initial position of the simulation is based on the supine position from the CT scan with the sacrum fixed. The flexion simulation transitions through a position corresponding to the neutral upright seated position. Maximum flexion is reached when the motion stabilizes.
To achieve extension in the seated position, the multifidi and quadratus lumborum must be contracted with a max force of 1000N (CSA 750cm2).
Bone contacts, along with ligament and passive muscle strains, constrain the vertebrae between L1 (under force displacement) and the fixed sacrum. Thus, the vertebrae in neutral and extension simulated positions are exported, and the sagittal parameters are calculated (aSim).

2.2 Statistical analysis
Statistical analysis was carried out with XLStat software using Wilcoxon non-parametric tests with a significance threshold of $p<0.005$.

3. Results and discussion

No significant differences were found between angles measured from MRI, registered and simulated vertebrae for neutral and extension as shown in table 1.

***Table 1**. Intervertebral angles (IVA) and Lumbar Lodosis (LL) obtained in two different conditions: neutral and extension sitting.*
credit: M.Pissonnier

		Neutral sitting			Extension sitting		
		aMRI	aReg	aSim	**aMRI**	aReg	aSim
IVA	L1-L2	**2.74**	1.32	1.76	**4.48**	7.62	4.01
	L2-L3	**0.61**	1.78	3.25	**5.1**	8.55	5.75
	L3-L4	**1.18**	3.02	2.67	**8.58**	9.73	9.82
	L4-L5	**1.35**	0.88	2.89	**11.92**	12.8	14.62
	L5-S1	**3.76**	5.98	3.89	**9.64**	10.95	13.46
LL (L1L5)		**15.09**	14.36	14.61	**60.7**	56.79	43.2
p value			*0.281*	*0.156*		*0,219*	*0,281*

† means value different from standard (MRI) with $p<0.05$

Total range of motion (ROM) is in accordance to Bogduk in L5-S1 intervertebral space as it stays the only one in lordosis even in flexion.
No comparison is possible regarding the ROM because our neutral reference is the active upright in vivo position and the closest model in literature (Remus et al. 2021) uses supine passive data as neutral (the upright position is done in vitro).
Measurements taken manually will require inter- and intra-observer analysis.

4. Conclusions

This specific subject model reproduces the neutral and extended lumbar positions in comparison with multi-position MRI according to the gold standard used by clinicians. However, it would be necessary to use the neutral seated position as the starting position for the movements instead of the supine one.
Further parametric studies will be needed to calibrate the model regarding active motion of the spine including the maximum flexion.

Conflict of Interest Statement

None

References

Perrier, A., Luboz, V., Bucki, M., Vuillerme, N., & Payan, Y. (2015). Conception and evaluation of a 3D musculoskeletal finite element foot model. Computer methods in biomechanics and biomedical engineering, 18 Suppl 1, 2024–2025. doi:10.1080/10255842.2015.1069606

Elyasi, E., Perrier, A., Bailet, M., & Payan, Y. (2022). Biomechanical lower limb model to predict patellar position alteration after medial open wedge high tibial osteotomy. Journal of biomechanics, 136, 111062. doi:10.1016/j.jbiomech.2022.111062

Bogduk, N. (2013). *Clinical and Radiological Anatomy of the Lumbar Spine* (Fifth ed). Elsevier.

Goel VK, Ramirez SA, Kong W, Gilbertson LG. Cancellous bone Young's modulus variation within the vertebral body of a ligamentous lumbar spine--application of bone adaptive remodeling concepts. J Biomech Eng. 1995 Aug;117(3):266-71. doi: 10.1115/1.2794180. PMID: 8618378.

Modi, H. N., Suh, S. W., Song, H. R., Yang, J. H., Kim, H. J., & Modi, C. H. (2008). Differential wedging of vertebral body and intervertebral disc in thoracic and lumbar spine in adolescent idiopathic scoliosis - A cross sectional study in 150 patients. Scoliosis, 3, 11. doi:10.1186/1748-7161-3-11

Remus, R., Lipphaus, A., Neumann, M., & Bender, B. (2021). Calibration and validation of a novel hybrid model of the lumbosacral spine in ArtiSynth-The passive structures. PloS one, 16(4), e0250456. doi:10.1371/journal.pone.0250456

Received date: *leave blank*
Accepted date: *leave blank*
Published date: *leave blank*
Volume: *leave blank*
Publication year: *leave blank*